



Fouling study on vacuum-enhanced direct contact membrane distillation for seawater desalination

Gayathri Naidu^a, Sanghyun Jeong^a, Saravanamuthu Vigneswaran^a, Eun-Kyung Jang^c, Yong-Jun Choi^b, Tae-Mun Hwang^{c,*}

^aFaculty of Engineering, University of Technology Sydney (UTS), P.O. Box 123, Broadway, NSW 2007, Australia

^bCivil Engineering Department, Kyungnam University, Masan 631-701, Korea

^cKorea Institute of Construction Technology, Gyeonggi-do 411-712, Republic of Korea, Tel. +82 31 910 0741; Fax: +82 31 910 0291; email: taemun@kict.re.kr (T.-M. Hwang)

Received 15 January 2015; Accepted 1 April 2015

ABSTRACT

Vacuum-enhanced direct contact membrane distillation (VE-DCMD) has been proposed to improve the DCMD system performance with better effective energy efficiency. However, the higher driving forces by the presence of vacuum pressure at permeate side of the VE-DCMD system could contribute to higher fouling development. In this study, thus, the biochemical fouling development of VE-DCMD with different vacuum pressures (700, 500, and 300 mbar) for seawater desalination was investigated in comparison with DCMD (1,000 mbar of pressure applied). VE-DCMD showed a significant increase in initial permeate flux while its flux decline was faster than DCMD. Low molecular weight (LMW) organics were found to be a dominant organic foulant on DCMD with thermally disaggregated humic substances (HS) to LMW HS-like organics. On the other hand, the presence of vacuum reduced the disaggregation HS to LMW HS-like organics. However, high driving force of VE-DCMD caused higher deposition of organic foulant including the LMW organics as well as HS. It also led to the higher LMW organic contents in permeate. Fluorescence excitation–emission matrix (F-EEM) analysis result showed that fulvic-like organic is a dominant HS foulant in VE-DCMD. Fouling development on membrane was observed using scanning electron microscope, contact angle, and confocal laser scanning microscope.

Keywords: Fouling; Humic substances; Low molecular weight organics; Seawater; Vacuum-enhanced DCMD

1. Introduction

Membrane distillation (MD) has been identified as an alternative technology for the application of seawater (SW) desalination [1]. MD is a membrane-

integrated thermal distillation process with transmembrane vapor pressure difference across a hydrophobic membrane as the driving force [2]. One of the most significant advantages of the MD process for desalination is the minimal effect of feed salt concentration on the performance of the system. Potentially, MD can achieve an almost zero liquid discharge, minimizing

*Corresponding author.

brine management for SW desalination. Direct contact membrane distillation (DCMD) is one of the most commonly used MD configurations due to its application simplicity and flexibility of the process to be carried out in any desired membrane configuration (flat sheet, spiral wound, capillaries, or hollow fibers) [3].

Recently, to maximize the productivity of DCMD system and enhance its capacity, various optimization approaches have been adopted such as increasing flow rate turbulence, usage of channel spacer, and improved configuration and heat exchangers [4,5]. It will make the performance of DCMD as competitive as other membrane processes such as reverse osmosis (RO) for SW desalination [5]. A larger temperature difference in DCMD can achieve higher water fluxes as vapor pressure increases exponentially with increasing temperature [6]. Similarly, in another study, optimized feed/permeate flow velocity enabled to increase the performance of the DCMD system with a 30% higher recovery ratio and 60% lower pumping energy [7]. In this regard, vacuum incorporation to DCMD is another approach that has been proposed to enhance the performance of DCMD. The initial concept of vacuum-enhanced DCMD (VE-DCMD) was proposed by Schofield et al. [8]. More recently two other studies presented the potential of VE-DCMD [9,10]. Cath et al. [9] demonstrated that the VE-DCMD system achieved a 15% permeate flux increment (compared to DCMD) with the reduction of permeate side pressure (increased vacuum) from 108 to 94 kPa. Importantly, this study highlighted that from an economic aspect, the incorporation of vacuum does not incur significant additional cost due to the low pressure gradient on the pump. In another study, Martinetti et al. [10] reported that a reduced permeate pressure from 660 mmHg (abs) to 360 mmHg (abs) in DCMD resulted in the increased initial flux from around 35 to 40 L m⁻² h⁻¹ (LMH) at the same temperature difference of 40°C. Overall, these studies have proven that the VE-DCMD configuration was effective in improving the performance of systems with minimal additional cost. Further, the presence of vacuum (in VE-DCMD) reduced conductive heat loss through the membrane, which is the major energy inefficiency of DCMD operation [8,9,11,12]. Hence, the incorporation of vacuum to the DCMD unit would also enable to improve the energy efficiency of the system, apart from enhancing the overall performance of the DCMD operation.

On the other hand, the higher driving force of the VE-DCMD system could potentially contribute to higher fouling development. In fact, the DCMD study conducted with RO brine as the feed solution

observed that higher flux decline related to scaling with higher presence of vacuum at 360 mmHg (abs) permeate pressure compared to at 660 mmHg (abs) permeate pressure [10]. This was attributed to the higher concentration polarization at the feed–membrane interface with increased driving force. However, thus far, no detailed study has been carried out on the relationship between increased driving force and membrane fouling in MD.

The aspect of fouling in DCMD with SW has been analyzed based on declining distillate flux and increased distillate conductivity [13–15]. Shirazi et al. [13] reported on the higher distillate flux reduction with real SW as a feed solution compared to synthesized SW. This was attributed to the prevalent formation of membrane fouling by mixed organic constituents in the real SW. Similarly, Hsu et al. [14] observed the gradual flux decline in DCMD with SW pretreated by ultrafiltration, attributed to the organic contents in the SW. Recently, Naidu et al. [16] carried out a detailed characteristic of organic compound behavior in DCMD to treat SW based on the liquid chromatogram organic carbon detector (LC-OCD) analysis. This study showed that humic substances (HS) and low molecular weight (LMW) organics are the dominant organic foulants in SW. Contrarily, biopolymer is not a significant organic foulant in MD SW operation due to its low concentration in SW and its hydrophilic nature. HS absorb more favorably onto hydrophobic membrane surfaces due to its hydrophobic nature [16,17]. Further, it was highlighted that HS showed a tendency to thermally disaggregate to LMW humic organics. The presence of the LMW humic organics was related to the increase in biofouling potential. In this regard, it is worth studying the behavior of humic-like organics as a dominant foulant in MD. Fluorescence excitation–emission matrix (F-EEM) is a rapid, selective, and sensitive analysis tool that can be used to determine the humic-like and fulvic-like contents in the feed solution [18].

Hence, in this study, the detailed fouling analysis of VE-DCMD was investigated for SW desalination in comparison with DCMD. The study intends to demonstrate the effectiveness of VE-DCMD in terms of performance enhancements while considering the biochemical fouling development. This would enable to provide detailed insights on the application of the VE-DCMD system for SW desalination as well as to represent the influence of driving force on MD fouling development. For this purpose, LC-OCD analysis was used for detailed organic characterization. F-EEM technique was adopted to determine the dominant humic-like foulant in SW MD. Further, fouled

membrane observation was carried out using scanning electron microscope (SEM), contact angle, and confocal laser scanning microscope (CLSM) analyses.

2. Material and methods

2.1. Experimental setup

2.1.1. DCMD and VEDCMD setup

Fig. 1 presents a (a) bench-scale DCMD system and a (b) VE-DCMD system used in this study. Feed solution was heated at the set temperature in a sealed feed tank encased in an electric heating blanket. The temperature of the permeate side was regulated by a cooling unit. Initially, 2 L of feed solution and 2 L of cooling water were circulated into the membrane module by a peristaltic pump until a stable temperature is reached. The temperature of the feed solution and cooling water was measured at the inlet and outlet of the membrane module with temperature sensors. The hydraulic pressure on the feed inlet and permeate side outlet was measured with pressure gauges. The feed and permeate tanks were placed on electronic balances to monitor the permeate production and feed reduction over time. Each experiment was carried out until the feed volume was reduced to 0.4 L. Accordingly, the experimental duration ranged between 3.5 and 7.0 h based on the time required to achieve this feed volume reduction.

2.1.2. Membrane

A hydrophobic polytetrafluoroethylene flat-sheet hydrophobic membrane (General Electrics, US) was used in this study. The membrane support layer was made of polypropylene. The effective membrane area was 0.0168 m^2 ($0.21 \text{ m} \times 0.08 \text{ m}$). The dimensions of membrane cell channel were 21.0 cm (length), 8.0 cm (width), and 0.4 cm (height). The porosity, normalized pore size, and thickness of membrane provided by the supplier were 70–80%, 0.2, and $179 \mu\text{m}$, respectively.

2.1.3. Feed solution

Experiments were conducted with actual SW. It was collected from 1 m below the sea surface level at Chowder Bay in Australia. It was filtered through $140\text{-}\mu\text{m}$ centrifuge filtration system to remove all large particles. The SW properties include pH at 7.9–8.2, conductivity at around $51.8\text{--}55.5 \text{ ms cm}^{-1}$, total suspended solids in the range of $3.4\text{--}3.6 \text{ mg L}^{-1}$, while the salinity and turbidity were around 35.5 g/L and 0.40 NTU , respectively.

2.2. Fouling investigation

In a previous study, the MD setting was optimized using DI water in the range of $0.3\text{--}2.2 \text{ m s}^{-1}$ of flow velocities in terms of permeate flux, recovery ratio, and pumping energy [7]. A suitable operational setting was identified at a flow velocity of 1.1 m s^{-1}

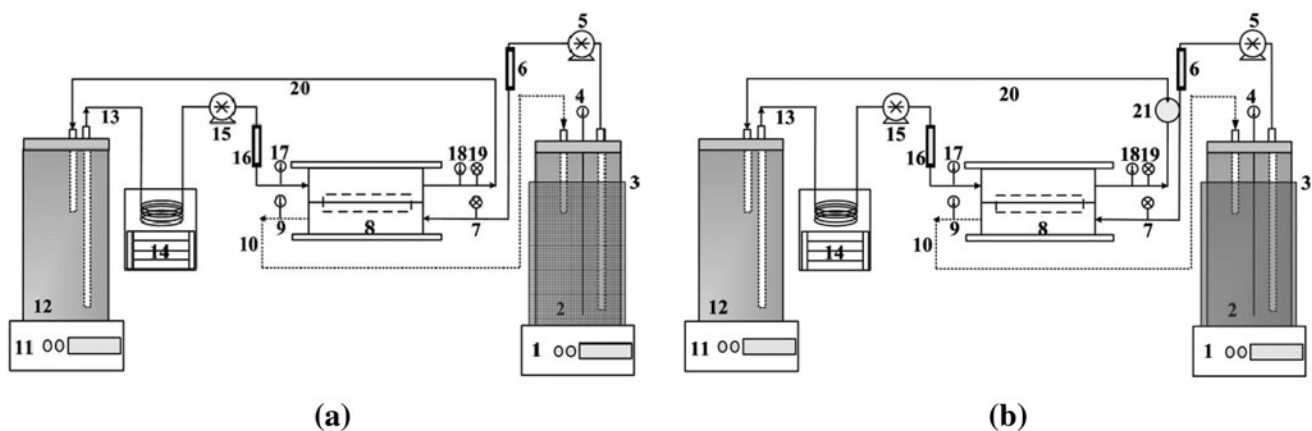


Fig. 1. Experimental setup of (a) DCMD and (b) VE-DCMD: (1) feed electronic balance, (2) feed tank, (3) heating blanket, (4) feed tank temperature sensor, (5) feed pump, (6) feed flowmeter gauge, (7) feed inlet pressure gauge, (8) membrane module, (9) feed outlet (brine) temperature sensor, (10) brine, (11) permeate electronic balance, (12) permeate tank, (13) cooling water, (14) cooling unit, (15) cooling pump, (16) cooling flowmeter gauge, (17) cooling water inlet temperature sensor, (18) cooling water outlet temperature sensor, (19) cooling water outlet pressure gauge, (20) permeate, and (21) vacuum pump.

($Re = 4,950$) and a feed temperature of 70°C , achieving a permeate flux of 35.7 LMH [7]. Thus, in this study, optimal condition (a feed and permeate flow velocity of 1.1 m s^{-1} , with feed and permeate temperatures of 70 ± 0.2 and $24 \pm 0.2^\circ\text{C}$, respectively) was used in the MD operation. VE-DCMD experiments were conducted with different vacuum pressures (700, 500, and 300 mbar) and without vacuum (which is same as DCMD and 1,000 mbar of pressure applied).

The corresponding volume of decreased feed water (L) and produced permeate (L) with the operation time (h) and membrane area (m^2) was used to calculate the experimental permeate flux in $\text{L m}^{-2} \text{ h}^{-1}$ (LMH). Meanwhile, the permeate flux was expressed as a function of feed volume concentrate factor (VCF). The VCF is defined as the ratio of feed volume (L_f) to concentrate volume (L_c), representing extend of volume concentration of feed as defined by other studies [7].

2.2.1. LC-OCD

The detailed organic characterization was done using LC-OCD (developed by Dr Huber) [19]. In this analysis, the organic fractions of the feed solution and membrane foulant were determined as DOC concentration. The size exclusion chromatography column in the LC-OCD system separates the organic fractions (Biopolymers; BP, humic substances; HS, building blocks; BB, and low molecular weight (LMW) organics were fractionated from DOC) according to their molecular size during the retention time. The separated compounds are detected by a ultra-violet (UV) detector (absorption at 254 nm) and an OCD detector (after inorganic carbon purging). The organic matter fractions are identified and quantified based on the size of the molecules. The LC-OCD system utilized a Toyopearl TSK HW50S column (TOSOH Bioscience GmbH, Stuttgart, Germany), with phosphate buffer mobile phase of pH 6.4 ($2.6 \text{ g L}^{-1} \text{ KH}_2\text{PO}_4$ and $1.5 \text{ mol L}^{-1} \text{ Na}_2\text{HPO}_4$) at a flow rate of 1.1 mL min^{-1} . After each experiment, the MD membrane was cut into small parts and placed in a beaker with milli-Q water. The beaker was sonicated to extract the organic residues on the MD membrane. The sonication was carried out with an ultrasonic bath (Powersonic 420, Thermoline Scientific, 300 W) for a short time (10 min) to prevent organic matter from denaturing. All samples were filtered through a $0.45\text{-}\mu\text{m}$ syringe filter prior to LC-OCD analysis.

2.2.2. Fluorescence excitation–emission matrix

In this study, humic-like as well as fulvic-like organic materials in the feed solution before and after DCMD operation were characterized using F-EEM. Fluorescence measurements were carried out for dissolved organic matter in water samples using a Varian Eclipse Fluorescence Spectrophotometer as explained in the detailed analysis study by Jeong et al. [18]. Two characteristic peaks for humic-like and fulvic-like were usually observed in EEMs including Peak A—humic-like (ex/em = $250\text{--}260/380\text{--}480 \text{ nm}$) and Peak C—fulvic-like (ex/em = $300\text{--}370/400\text{--}500 \text{ nm}$).

2.2.3. Field emission scanning electron microscope

The morphology and composition of the deposit layer formed on the membrane were analyzed using Zeiss Evo LS15 field emission scanning electron microscope (FE-SEM). The fouled membrane coupons were dried in a desiccator and analyzed without any further treatment. Both the top surface and the cross-section of the fouled membrane coupons were analyzed. They were mounted on a holder using double-sided carbon tape.

2.2.4. Contact angle measurement

The contact angle of membrane surface was measured to determine the change of hydrophobicity of the membrane surface. This measurement was carried out by sessile drop method using a goniometer (Theta Lite). The images were captured and interpreted by One Attention Image Advanced software. The shape of a liquid droplet is determined by the surface tension of the liquid. To form a water drop ($1.8\text{--}2.0 \text{ mL}$ of milli-Q water) on the dried membrane surface, a milliliter syringe was used. Measurements were repeated five times and the average values were reported in this study.

2.2.5. Confocal laser scanning microscope

In this study, the distributions of cells (nucleic acid) and biopolymers (polysaccharide) on MD membrane were investigated. They were observed using Olympus FV-1200 confocal laser scanning microscope (CLSM) after staining with 4',6-diamidino-2-phenylindole (DAPI, Sigma-Aldrich) and Concanavalin A (ConA, Molecular Probes), respectively. The number of live and dead cells in the fouled membrane was measured by staining the samples

with SYTO9 and propidium iodide (PI) as used in the previous study [20,21].

The fouled membrane samples were soaked in the working solutions of the stains, and incubated for 0.5 h in the dark at room temperature and rinsed with the corresponding buffer solution before microscopic observation. Their average biovolumes were obtained through three-dimensional (3D) objects counter in Fiji software following the Ref. [21]. This essentially involved calculating the volume (μm^3) of the voxels (volumetric pixels) belonging to each object with the total volume of the biofilm being the sum volume of all the objects. The biovolume ($\mu\text{m}^3 \mu\text{m}^{-2}$) was the total volume (μm^3) per area (μm^2).

3. Results and discussion

3.1. Permeate flux

Fig. 2 presents the permeate flux pattern of VE-DCMD with different vacuum pressures, ranged from 1,000 to 300 mbar. Compared to DCMD, the incorporation of vacuum (VE-DCMD) led to significant increase in initial permeate flux, from $17.44 \text{ L m}^{-2} \text{ h}^{-1}$ (LMH) at 1,000 mbar up to 27.59 LMH at 300 mbar. Even with slight vacuum (at 700 mbar), the initial permeate flux was increased to 20.49 LMH. This clearly showed that the incorporation of vacuum to the DCMD system increased the initial permeate flux effectively. Similarly, previous VE-DCMD studies highlighted the improvement of permeate flux as vacuum pressure increased [9,10].

Although the higher vacuum pressure resulted in the higher permeate flux, it reduced permeate flux rapidly as shown in Fig. 2. At 1,000 mbar (DCMD), a gradual permeate flux reduction was observed with a

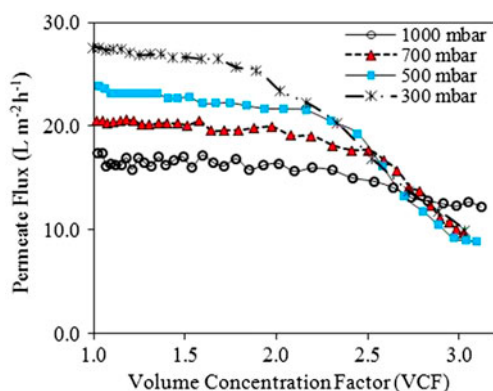


Fig. 2. Permeate flux pattern in VE-DCMD (to treat seawater) operated with different vacuum pressures ($T_f = 70^\circ\text{C}$, $T_p = 24^\circ\text{C}$, v_f and $v_p = 1.1 \text{ m/s}$).

total permeate flux reduction of 31.7%. Comparatively, as the vacuum pressure was increased, from 700 to 300 mbar, a sharp permeate flux decline pattern was observed at VCF 2.75 for 700 mbar, VCF 2.5 for condition 500 mbar, and VCF 2.0 for condition 300 mbar. With 300 mbar, a 64.1% of total permeate flux reduction was found while less permeate flux decline (31.7%) was observed with 1,000 mbar. This faster permeate flux reduction trend could be attributed to the fouling pattern of the different vacuum pressures with different driving forces and mass transfers. Therefore, this study carried out a detailed fouling analysis in VE-DCMD with different vacuum pressures in the following section.

3.2. Detailed organic analysis

In this study, the variation of organic matter in the feed solution of the VE-DCMD operation as well as the organic characteristics in the permeate solution and membrane foulant was analyzed using LC-OCD analysis.

Based on the LC-OCD analysis, the initial organic contents in the SW (at VCF 1.0) contained mainly of HS (0.51 mg L^{-1}) and LMW organics (0.80 mg L^{-1}), with smaller portions of BP (0.07 mg L^{-1}) and BB (0.003 mg L^{-1}). In this study, BP and BB were not considered due to its small portions in DOC. The changes of organic compounds (mainly HS and LMW organics) in the feed solution during the operation of VE-DCMD were investigated from VCF 1.0 to VCF 3.0 with the presence of vacuum.

3.2.1. Characteristics of organics in the feed solution and in the permeate

It was observed that with 1,000 mbar (DCMD), both the HS and LMW organics increased with VCF. However, the concentration of HS did not increase proportionally with VCF, while the concentration of LMW organics increased twofolds higher than expected at VCF 3.0. The similar trend was observed in a previous study by Naidu et al. [16]. It was highlighted that under thermal DCMD operation, HS showed a tendency to thermally be disaggregated to LMW humic-like organics, and therefore increased the contents of LMW organics in the feed solution.

On the other hand, the presence of vacuum varied the pattern of organic contents in the feed solution. HS content was not changed significantly in the feed solution when it compared at VCF 1.0 and VCF 3.0. It showed that the change of HS to LMW HS-like in VE-DCMD was slightly compared to that in DCMD.

Instead of that, vacuum resulted in more HS fouling on membrane. However, its content was relatively low than LMW organics. In the case of LMW organics, their content decreased in the final feed solution (at VCF 3.0) compared with the initial feed solution (at VCF 1.0). This indicates that LMW organics are a dominant foulant on membrane in VE-DCMD. Evidently, significantly higher portion of organic was deposited on the membrane with the presence of vacuum (700–300 mbar) (Table 1). Therefore, the results suggested that the higher driving force led to more LMW organics adhered onto the membrane.

Further, LMW organics were mainly detected in the final permeate solution with the pattern of concentration increase in DOC as well as LMW organics as vacuum pressure increased. This showed that increased driving force by vacuum pressure caused more penetration of LMW organics to permeate side. In the end, the results highlighted that the increased vacuum pressure influenced the organic fouling pattern in VE-DCMD.

3.2.2. Characteristics of organic foulants on the membrane

Mass of organic deposited on the membrane was calculated with the difference between DOC concentration of the feed solution at VCF 1.0 (initial feed volume = 2 L) and DOC concentration of the feed solution at VCF 3.0 (final feed volume = 0.667 L) as well as DOC concentration of final permeate solution (Table 1). In this regard, the LC-DOC results showed that around 0.007–0.069 mg L⁻¹ of organic concentration was detected in the final permeate solutions as shown in Table 1. The organic concentration of permeate showed an increasing trend with increased vacuum pressure.

Based on the DOC concentration of the initial and final feed solution, the DCMD (1,000 mbar of permeate

pressure) showed around 0.159 mg was reduced in organic mass of the feed solution. Meanwhile, around 0.023 mg of organic mass was detected on the permeate solution. Hence, the organic mass deposited on the membrane area was calculated to be 16.1 mg cm⁻² (Table 1). Comparatively, at condition IV (300 mbar), a significantly higher organic mass was deposited on the membrane at 58.1 mg cm⁻². The amount of organic deposited on membrane after operation of VE-DCMD increased with the increased vacuum pressure.

3.3. Characterization of HS in VE-DCMD

In this study, detailed characterization of HS (which is a dominant foulant on MD) was carried out using F-EEM analysis. The F-EEM technique is a rapid, selective, and sensitive and offers information regarding the fluorescence characteristics of compounds by changing the excitation and the emission wavelength simultaneously.

In this study, for quantitative analysis, the average value of fluorescence intensities in the range of ex/em of each peak was used in comparison to relative abundance of standard organics (humic-like—humic acid; HA, and fulvic-like—fulvic acid; FA). In order to establish the standard curve, 0.25, 0.5, 1.0, and 2.0 mg/L of each model compound were used. As expected, in the case of HA, “A” peak has a good correlation with HA concentration. Thus, “A” peak indicates the HA-like peak and a following relationship were established: humic-like mg-HA/L = 0.51 × “A” peak intensity. Similarly, “C” peak showed the highest intensity of fulvic acid (FA) and with increase in FA, fluorescence intensity increased. Thus, “C” peak compounds to fulvic-like peak and the relationship is fulvic-like mg-FA/L = 0.48 × “C” peak intensity. From the above relationships established, values for humic-like and fulvic-like were calculated to mg-HA/L and mg-FA/L, respectively.

Table 1
Organics fouling pattern under VE-DCMD operation with different vacuum pressures

Vacuum pressure (mbar)	Organic concentration (mg L ⁻¹)									Organic deposited on membrane (mg cm ⁻²)
	Initial feed solution (VCF 1.0)			Final feed solution (VCF 3.0)			Final permeate solution			
	DOC	HS	LMW ^a	DOC	HS	LMW ^a	DOC	HS	LMW ^a	
1,000	1.073	0.480	0.405	2.980	0.818	1.928	0.007	0.001	0.006	16.1
700	1.090	0.475	0.404	2.553	1.383	1.062	0.025	0.002	0.022	46.9
500	1.056	0.391	0.469	2.302	1.127	1.062	0.042	0.004	0.036	52.0
300	1.095	0.394	0.490	2.207	1.131	1.02	0.069	0.007	0.057	58.1

^aLMW: Low molecular weight organics.

In natural water sources, HS generally comprises humic-like and fulvic-like organic materials with more prevalent fulvic contents [22]. F-EEM analysis displayed a higher concentration of fulvic-like organics in SW used in this study. Humic-like and fulvic-like organics in SW were 0.23 mg-HA/L and 0.45 mg-FA/L, respectively.

As vacuum pressure increased, the concentrations of humic-like and fulvic-like organics in the feed solution decreased (Fig. 3(a) and (b)). This indicated that the presence of vacuum resulted in more humic fouling on membrane in DCMD. In DCMD (at 1,000 mbar), the concentrations of humic-like and fulvic-like organics increased with the decrease in the feed solution volume from VCF 1.0 to VCF 2.0. This showed that there was a slight deposition of HS during the initial filtration time of DCMD. On the other hand, between VCF 2.0 and VCF 3.0, high rate of HS fouling was observed in DCMD. This was found from the slight increase in the concentrations of humic-like and fulvic-like organics in the feed solution. In the case of VE-DCMD, humic-like organics fouling occurred from the initial stage of operation (VCF 1 to VCF 2). Furthermore, its tendency increased as vacuum pressure increased. However, adhesion of humic-like organic on membrane of VE-DCMD decreased with the increase in vacuum pressure. This similar and remarkable pattern was observed from the trend of fulvic-like organic concentration in the feed solution at VCF increased (Fig. 3(b)). This indicated that the changes in the humic contents as well as extend of humic adhesion onto the membrane occurred from VCF 2.0 onwards. This similar trend was observed with the LC-OCD results. Meanwhile, the mass of humic-like and fulvic-like foulant in DCMD and VE-DCMD increased with the increase in vacuum pressure and as the feed solution concentration decreased gradually (Fig. 3(c)). The result showed that fulvic-like organic is a dominant HS foulant. FAs are LMW HS, generally less aromatic and higher oxygen content than other HSs, which means more reactive. HS are only soluble in water at certain pH levels, while FAs are soluble in water at all pH levels [23,24].

3.4. Fouled membrane observation

3.4.1. Field emission scanning electron microscope

The morphology of fouled MD membrane after running till VCF 3.0 with different vacuum pressures was observed using FE-SEM (Fig. 4). The results revealed that at 300 mbar of vacuum pressure in the

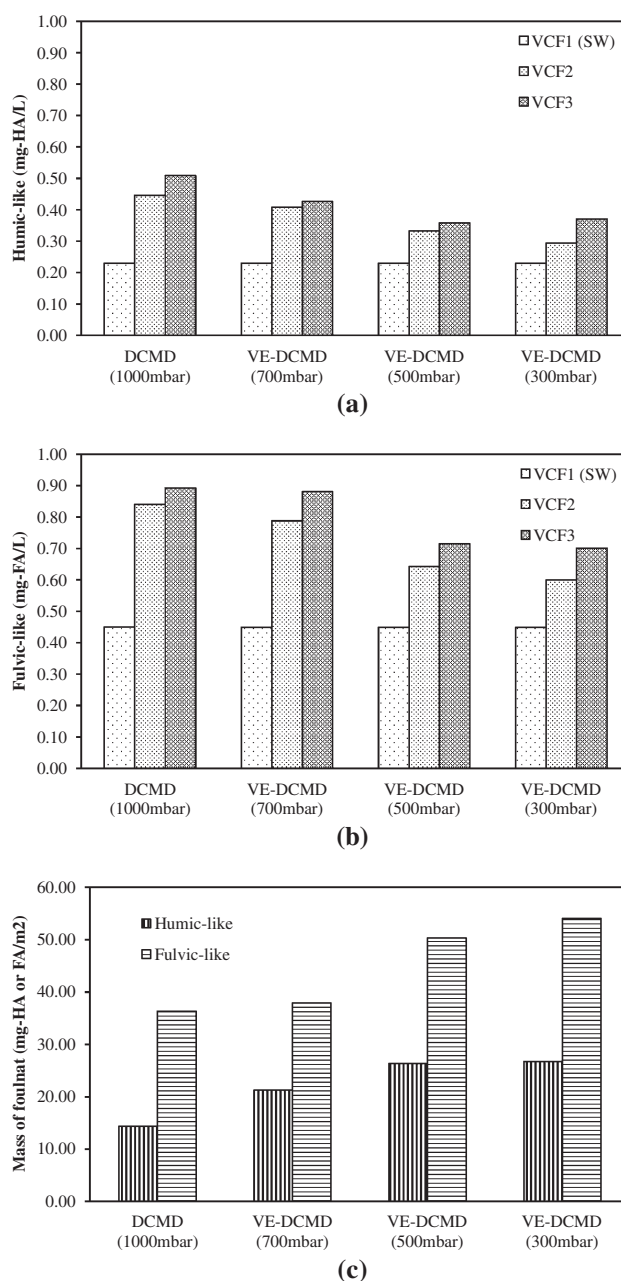


Fig. 3. Variation of (a) humic-like and (b) fulvic-like organic concentrations in feed solution (obtained from F-EEM analysis) during operational time (VCF1–VCF3), and (c) mass of humic-like and fulvic-like foulant in DCMD and VE-DCMD (it was obtained from mass balance calculation between VCF3 and VCF1).

VE-DCMD system, higher foulant coverage presented across the membrane surface compared to the DCMD system. In terms of membrane cross-section, the higher driving force at 300 mbar appeared to have compressed the membrane.

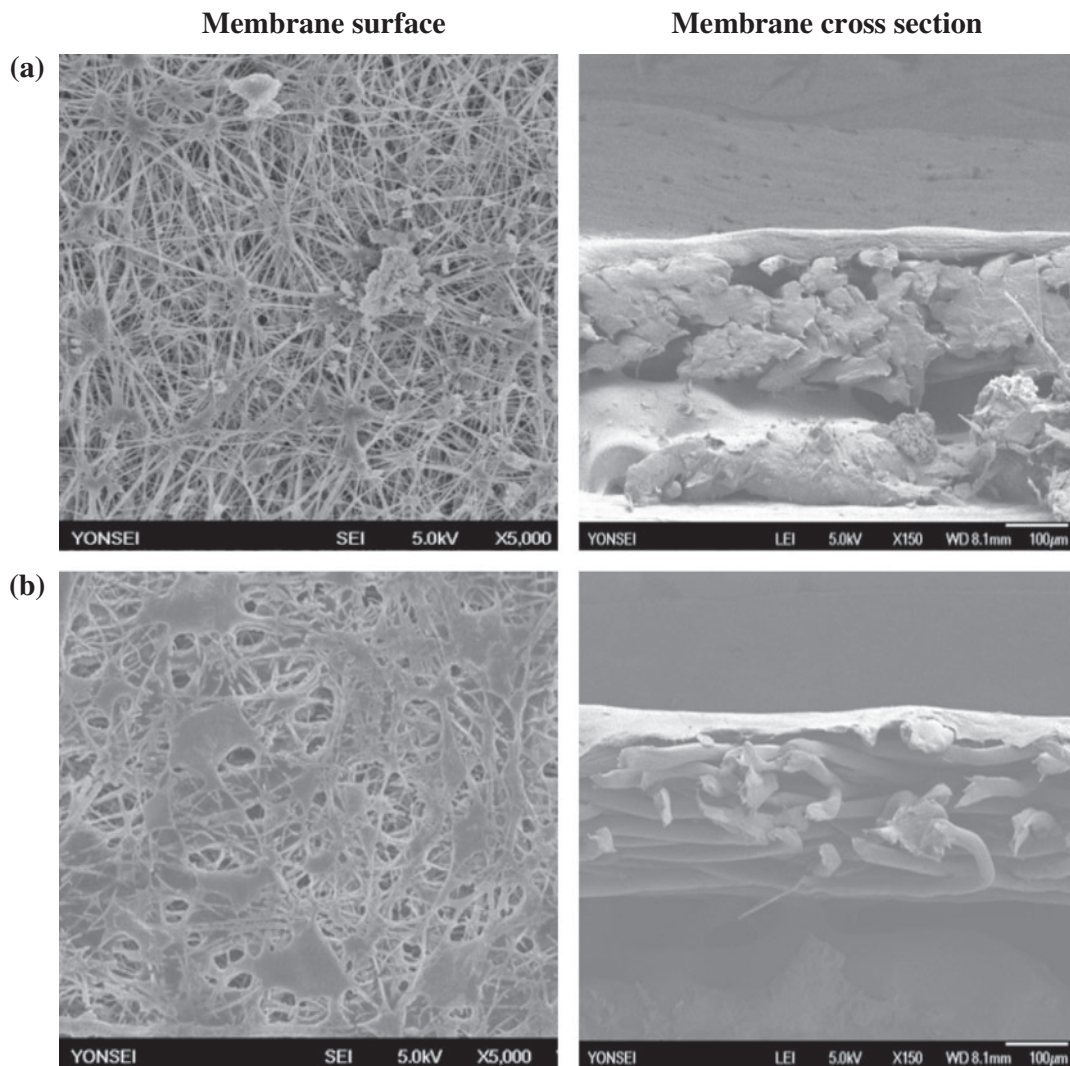


Fig. 4. SEM images of membrane surface and cross-section for (a) DCMD (at 1,000 mbar) and (b) VE-DCMD (at 300 mbar of vacuum pressure).

3.4.2. Contact angle

The change of hydrophobicity of fouled membrane was examined by measuring the contact angle. The results showed a reduction of contact angle with increased vacuum pressure. The contact angle of fouled membrane at vacuum pressure of 1,000 mbar was 133.7° while this decreased to 127.5° at 300 mbar. The results suggest that the increased vacuum pressure led to more foulant deposition on the membrane, reducing the hydrophobicity of the membrane surface. One of the major consequences of reduced membrane hydrophobicity is membrane wetting [25]. Hence, in this study, the reduced membrane hydrophobicity could be related to the increase in permeate organic

contents as observed in the LC-OCD analysis presented in Table 1.

3.4.3. Biofilm observation

Fig. 5 represents the average biovolume of cells and PS, and cell viability on fouled membrane. Biofilm formation (on fouled MD membrane) was observed with CLSM after DAPI staining for DNA and ConA staining for polysaccharide (PS) or biopolymers. The cell viability (the ratio of live cells to total cells) of the biofilm on fouled membranes was measured by staining with SYTO9 (live cells) and propidium iodide (PI) (dead cell).

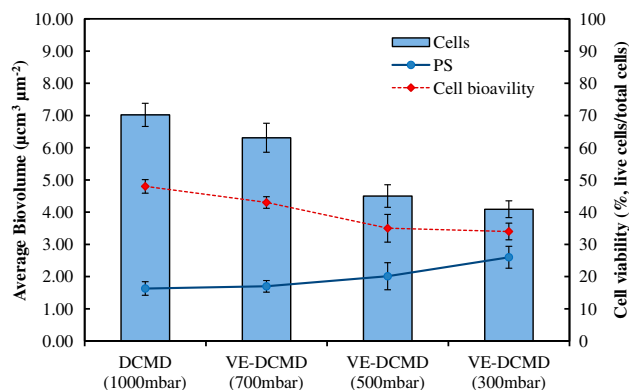


Fig. 5. Average biovolume of cells and PS, and cell viability on fouled membrane.

The PS concentration on fouled membrane of DCMD was $1.63 \pm 0.21 \mu\text{m}^3 \mu\text{m}^2$. However, as observed in organic foulant analysis, PS distribution on VE-DCMD increased with the increased vacuum pressure ($2.60 \pm 0.34 \mu\text{m}^3 \mu\text{m}^2$ with 300 mbar of vacuum pressure). However, the adhesion of cells on membrane and cell viability decreased as vacuum pressure increased. This indicated that the fouling mechanism of cells on membrane of VE-DCMD affected by the presence of vacuum. Therefore, further study is needed on the biofouling in VE-DCMD.

4. Conclusion

VE-DCMD showed a higher permeate flux compared to DCMD due to higher driving force by the presence of vacuum pressure at permeate side of the system and the lowered heat loss. However, these traits contributed on different fouling behaviors. Likewise DCMD, LMW organics are the dominant organic foulants of VE-DCMD, although the thermal disaggregation of HS to LMW HS-like organics decreased in VE-DCMD. As vacuum pressure increased in VE-DCMD, the organic foulant deposition increased with high content of LMW organics. HS were investigated in detail using F-EEM analysis. It showed that fulvic-like organics were the main foulant in HS foulant. Furthermore, more LMW organics were observed in the final permeate solution after operating VE-DCMD with higher vacuum pressure. More organic deposition was also observed in SEM analysis, and hydrophobicity (obtained from contact angle measurement) was increased with more organic deposition. The presence of vacuum also affected the biological fouling on membrane of VE-DCMD.

Acknowledgments

This research was supported by a grant (code 13IFIP-B065893-01) from Industrial Facilities & Infrastructure Research Program funded by Ministry of Land, Infrastructure and Transport of Korean government and a grant from a Strategic Research Project (20140030-1-1) funded by Korea Institute of Construction Technology.

References

- [1] M.R. Qtaishat, F. Banat, Desalination by solar powered membrane distillation systems, *Desalination* 308 (2013) 186–197.
- [2] M. Khayet, Membranes and theoretical modeling of membrane distillation: A review, *Adv. Colloid Interface Sci.* 164 (2011) 56–88.
- [3] S. Al-Obaidani, E. Curcio, F. Macedonio, G. Di Profio, H. Al-Hinai, E. Drioli, Potential of membrane distillation in seawater desalination: Thermal efficiency, sensitivity study and cost estimation, *J. Membr. Sci.* 323 (2008) 85–98.
- [4] M.S. El-Bourawi, Z. Ding, R. Ma, M. Khayet, A framework for better understanding membrane distillation separation process, *J. Membr. Sci.* 285 (2006) 4–29.
- [5] R.B. Saffarini, E.K. Summers, H.A. Arafat, J.H. Lienhard V, Technical evaluation of stand-alone solar powered membrane distillation systems, *Desalination* 286 (2012) 332–341.
- [6] J. Zhang, N. Dow, M. Duke, E. Ostarcevic, J. Li, S. Gray, Identification of material and physical features of membrane distillation membranes for high performance desalination, *J. Membr. Sci.* 349 (2010) 295–303.
- [7] G. Naidu, S. Jeong, S. Vigneswaran, Influence of feed/permeate velocity on scaling development in a direct contact membrane distillation, *Sep. Purif. Technol.* 125 (2014) 291–300.
- [8] R.W. Schofield, A.G. Fane, C.D.J. Fell, Factors affecting flux in membrane distillation, *Desalination* 77 (1990) 279.
- [9] T.Y. Cath, V.D. Adams, A.E. Childress, Experimental study of desalination using direct contact membrane distillation: A new approach to flux enhancement, *J. Membr. Sci.* 228 (2004) 5–16.
- [10] C.R. Martinetti, A.E. Childress, T.Y. Cath, High recovery of concentrated RO brines using forward osmosis and membrane distillation, *J. Membr. Sci.* 331 (2009) 31–39.
- [11] S. Bandini, C. Gostoli, G.C. Sarti, Role of heat and mass transfer in membrane distillation process, *Desalination* 81 (1991) 91.
- [12] J. Koo, J. Han, J. Sohn, S. Lee, T. Hwang, Experimental comparison of direct contact membrane distillation (DCMD) with vacuum membrane distillation (VMD), *Desalin. Water Treat.* 51 (2013) 6299–6309.
- [13] M.M.A. Shirazi, A. Kargari, D. Bastani, L. Fatehi, Production of drinking water from seawater using membrane distillation (MD) alternative: Direct contact MD and sweeping gas MD approaches, *Desalin. Water Treat.* 52 (2014) 2372–2381.

- [14] S. Hsu, K. Cheng, J. Chiou, Seawater desalination by direct contact membrane distillation, *Desalination* 143 (2002) 279–287.
- [15] K. He, H.J. Hwang, M.W. Woo, I.S. Moon, Production of drinking water from saline water by direct contact membrane distillation (DCMD), *J. Indust. Eng. Chem.* 17 (2011) 41–48.
- [16] G. Naidu, S. Jeong, S. Vigneswaran, Interaction of humic substances on fouling in membrane distillation for seawater desalination, *Chem. Eng. J.* 262 (2015) 946–957.
- [17] C. Jucker, M.M. Clark, Adsorption of aquatic humic substances on hydrophobic ultrafiltration membranes, *J. Membr. Sci.* 97 (1994) 37–52.
- [18] S. Jeong, S. Kim, C. Min Kim, S. Vigneswaran, T. Vinh Nguyen, H. Shon, J. Kandasamy, I. Kim, A detailed organic matter characterization of pretreated seawater using low pressure microfiltration hybrid systems, *J. Membr. Sci.* 428 (2013) 290–300.
- [19] S.A. Huber, A. Balz, M. Abert, W. Pronk, Characterisation of aquatic humic and non-humic matter with size-exclusion chromatography—organic carbon detection—organic nitrogen detection (LC–OCD–OND), *Water Res.* 45 (2011) 879–885.
- [20] S. Jeong, L. Kim, S. Kim, T. Nguyen, S. Vigneswaran, I. Kim, Biofouling potential reductions using a membrane hybrid system as a pre-treatment to seawater reverse osmosis, *Appl. Biochem. Biotechnol.* 167 (2012) 1716–1727.
- [21] S. Jeong, S.A. Rice, S. Vigneswaran, Long-term effect on membrane fouling in a new membrane bioreactor as a pretreatment to seawater desalination, *Bioresour. Technol.* 165 (2014) 60–68.
- [22] P.G. Coble, Characterization of marine and terrestrial DOM in seawater using excitation–emission matrix spectroscopy, *Mar. Chem.* 51 (4) (1996) 325–346.
- [23] R.F. Chen, J.L. Bada, The fluorescence of dissolved organic matter in porewaters of marine sediments, *Mar. Chem.* 45 (1994) 31–42.
- [24] M.M.D. Sierra, M. Giovanela, E. Parlanti, E.J. Soriano-Sierra, Fluorescence fingerprint of fulvic and humic acids from varied origins as viewed by single-scan and excitation/emission matrix techniques, *Chemosphere* 58 (6) (2005) 715–733.
- [25] M. Gryta, M. Barancewicz, Influence of morphology of PVDF capillary membranes on the performance of direct contact membrane distillation, *J. Membr. Sci.* 358 (2010) 158–167.